Author(s): Miettunen, Kati & Halme, Janne & Lund, Peter

Title: Segmented Cell Design for Improved Factoring of Aging Effects in Dye Solar Cells

Year: 2009

Version: Post print

Please cite the original version:

Miettunen, Kati & Halme, Janne & Lund, Peter. 2009. Segmented Cell Design for Improved Factoring of Aging Effects in Dye Solar Cells. Journal of Physical Chemistry C. Volume 113, Issue 23. 10297-10302. ISSN 1932-7447 (printed). DOI: 10.1021/jp902974v.

Segmented Cell Design for Improved Factoring of Aging Effects in Dye Solar Cells

Kati Miettunen[*]*, Janne Halme, Peter Lund*

Advanced Energy Systems Group, Department of Applied Physics, Helsinki University of Technology, P.O. BOX 5100, FIN-02015 TKK, Finland

AUTHOR EMAIL ADDRESS: kati.miettunen@tkk.fi

RECEIVED DATE (to be automatically inserted after your manuscript is accepted if required according to the journal that you are submitting your paper to)

TITLE RUNNING HEAD: Segmented Cells in Aging of Dye Solar Cells

* Corresponding author: Telephone: +358 9 451 8253. Fax: +358 9 451 3195.

E-mail address: kati.miettunen@tkk.fi.

A new segmented cell design was applied to study the aging of dye solar cell with stainless steel (StS) photoelectrode substrate, in particular the role of electrolyte in the degradation. Photovoltaic characterization indicated that StS photoelectrode cells are subjected to rapid (within hours or days) performance degradation which did not occur in the StS counter electrode cells. Other complimentary techniques, open circuit voltage decay (OCVD) and electrochemical impedance spectroscopy (EIS), showed changes in the recombination at the photoelectrode / electrolyte interface. With the segmented cell method, we confirmed that the electrolyte was not contaminated by the StS nor was it subject to other significant changes related to the rapid degradation.

Introduction

Nanostructured dye solar cells (DSC) are promising low cost photovoltaic devices. The price of the cells could be reduced and suitability for mass production improved with new materials and techniques. In particular, the study of alternative substrate materials is highly motivated since traditionally used glass with transparent conductive oxide (TCO) layer constitutes about one third of the material costs of these cells.[1] Flexible stainless steel (StS) substrates are clearly cheaper compared to TCO glass [2,3] and also suitable for roll-to-roll mass production. StS has been used both as counter electrode (CE) [4-8] and photoelectrode (PE) substrate.[7,9-13] To gain flexible DSC, transparent polymer substrates are used with metal substrates. The preparation of efficient PEs with low temperature techniques required in the case of polymer substrate has proven out to be more difficult compared to that of CEs. Hence, the application of StS as a PE substrate is especially interesting. Indeed, the highest efficiency of flexible DSCs (8.6 %) has been achieved with StS as photoelectrode substrate.[13]

The stability of StS DSCs has been shown to be poorer compared to glass cells,[5,14] although StS substrates withstood electrolyte soaking tests.[4-6] The mechanisms resulting in the shorter lifetime are not, however, clear. Besides corrosion of the StS by the electrolyte,[8] it has also been suggested that there may be problems in the encapsulation[5] and that the StS substrate may contaminate the dyed TiO_2 layer with

harmful metal oxides.[15] In order to improve the stability, further clarification of the causes leading to the StS cell degradation is needed.

Aging is typically studied with photovoltaic characterization. A complimentary tool that allows decoupling the changes in different cell components is electrochemical impedance spectroscopy (EIS). When studying the stability of a component in electrolyte, electrolyte soaking tests followed by chemical composition analysis such as atomic absorption spectroscopy of the electrolyte are sometimes used.[4,6] Composition analysis is, however, restricted by the measurement accuracy. [4,6] In addition, analysis of the electrolyte requires dismantling of the cell and is thus not suitable for continuous examination of the cell degradation over long periods of time.

In this study we introduce a novel segmented cell method to decouple the aging effects in DSC. The segmented cell method is applicable for many different cases and its use is therefore presented in detail. Here, the method is applied to study the rapid degradation phenomenon observed in the StS PE cells. In addition to segmented cell method, photovoltaic characterization, open circuit voltage decay (OCVD), and electrochemical impedance spectroscopy (EIS) are applied to give complimentary insight. This study is focused on the electrolyte since it is a common cause of chemical instabilities and it might also act as contamination carrier. The purpose of this study is not to cover everything that may be connect to the aging of the StS PE cells but to give insight to the role of one cell component, the electrolyte.

Experimental methods

Segmented cell method. The idea of applying segment cell to aging studies is to separate the contribution of different cell components to the cell degradation. In a segmented cell, there are electrically isolated cell compartments that share the same electrolyte layer. We have previously employed a segmented cell structure for the examination of spatial performance distribution.[16] Some segmented structures have been used as an internal reference electrode [17] and for studying current leakage from a substrate.[18] Here, a 2-segment cell is adequate for the purpose of the investigation.

In general, a 2-segment cell for aging studies constitutes of a studied segment and a reference segment. Here, we connected a StS PE cell with a conventional glass cell as shown in Figure 1. As the two segments share the same electrolyte layer, differences in the electrolyte in the studied segment causes differences in the reference segment as well. In practice, the segmented cell method applied to degradation studies is a non-destructive way to detect changes in the electrolyte or depletion of charge carriers. More generally, it allows the monitoring of the long term stability of different kind of electrodes under influence of exactly same electrolyte and aging conditions.

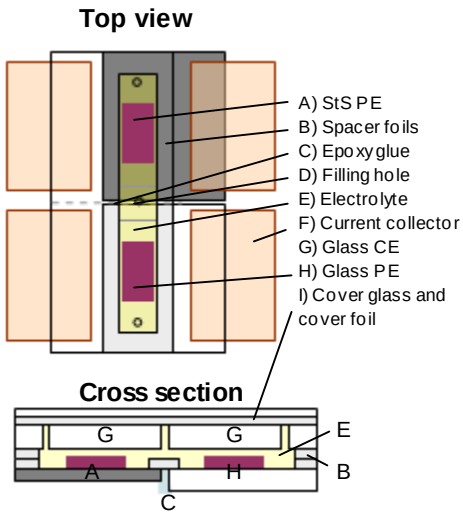

Figure 1. The structure of a 2-segment cell with StS PE and glass PE segments.

It should be noted that the segmented cell method can detect changes which are related to freely moving electrolyte components. Not all electrolyte components meet this criterion, for instance 4-*tert*-butylpyridine (4-*t*BP) adsorbs quickly to the TiO_2 surface resulting in an uneven electrolyte composition.[16] For this reason 2-segment cells with 4-*t*BP in the electrolyte need to be filled from the middle hole (Figure 1) in order to have similar electrolyte composition in both segments.

It should also be taken into account that when current is driven through one segment, the additional electrolyte reservoir in the one segment affects the charge transport in the other and vice versa. We

therefore expect that the segmentation method is most suitable for the study of relative differences such as detecting changes due to aging.

An important characteristic that needs to be determined for each segmented cell geometry and electrolyte is the time it takes for the changes in the electrolyte in the studied segment to affect the reference segment. This time is called here the response time. It depends on how quickly the electrolyte is mixed by diffusion. There is practically no convection in the DSCs and migration affects only charged particles. The response time can be determined both experimentally and by calculations as shown in the following chapters.

Experimental calibration of 2-segment cells. The response time of the segmented cell can be estimated experimentally by observing the motion of species that determine either optical or electrical properties of the cell segments, or both. Here, we determine the response time using 2-segment cells composed of a CE-CE segment with glass substrates and another segment with a copper substrate. Since all the triiodide that visit the segment with a copper substrate are immediately reduced to colorless ions,[4] we can study the response time by observing the loss of triiodide from the glass segment. The amount of triiodide in a cell is directly proportional to both the limiting current density [19] and the color of the electrolyte.[20] Polarization measurements showed that the limiting current density in the glass segment connected to a segment with a copper substrate decreased by half in one day. It can therefore be deduced that approximately half of the electrolyte species enter the other segment during one day. It should be noted that polarization of the cell may affect the distribution of triiodide and hence we recommend to minimize any polarization measurements during the calibration process. Note also that this response time estimate is valid only for this particular cell geometry and electrolyte.

Computational calibration of 2-segment cells. The response time can also be studied theoretically assuming that the mixing of the electrolyte follows the basic Fick's law of diffusion

$$\frac{\partial c}{\partial t} = D\nabla^2 c \qquad (1)$$

where c is the concentration of the studied particles, D is the diffusion coefficient of the particles, and t is the time. Let's assume that the concentration of studied particles in the measured segment is even c_{init} at the beginning of the experiment (t = 0) while the concentration in the reference segment is zero (c = 0), i.e. the initial state (t = 0) is a step function (Figure 2, t = 0). The concentrations start to even out between the measured segment and the reference segment when t > 0. Assuming infinite segments, the time evolution of the concentration profile is given by the follow the equation[21]

$$\frac{c(x,t)}{c_{init}} = \frac{1}{2}\left(1 + erf\left(\frac{x}{\sqrt{4Dt}}\right)\right). \quad (2)$$

We assume that the particles have similar D as the triiodide as in the experimental calibration. The D for triiodide in the electrolyte was $3.6 \cdot 10^{-6}$ cm^2/s as determined by limiting current density measurements.[22] Already after one day significant changes in the concentration at a distance of 1 cm from the boundary of the segments can be detected. The response time gained with these calculations is similar to that gained with the experimental calibration.

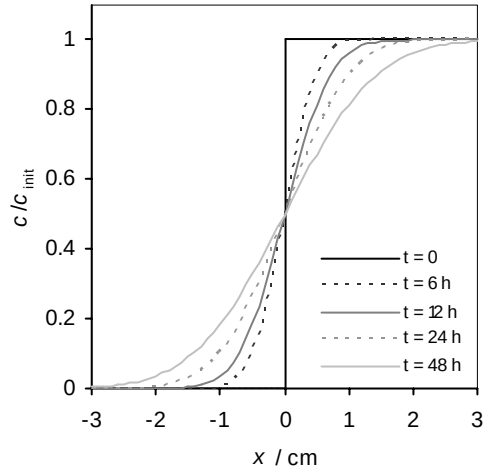

Figure 2. Concentration relative to c_{init} versus time. D = $3.6 \cdot 10^{-6}$ cm^2/s. The negative values of x represent the region of the reference segment and the positive values of x the studied segment.

Samples. The studied substrates were stainless steel 304 (thickness 1.25 mm, Outokumpu Ltd.) and fluorine-doped tin oxide (FTO) coated glass (thickness 2.5 mm, Pilkington TEC-15, sheet resistance 15 Ω/sq, Hartford Glass Company, Inc.).

In the PE preparation, commercial titania paste (Dyesol) was employed. The TiO_2 layers were sintered at 450 °C for 30 minutes followed by 16 hours of sensitization in a dye solution consisting of 0.32 mM *cis*-bis(isothiocyanato)bis(2,2'-bipyridyl-4,4'-dicarboxylato)-ruthenium(II) bis-tetrabutylammonium (Solaronix SA) in ethanol (99.5 wt-%). The CEs were thermally platinized [23] at 385 °C for 15 min using 5 mM tetrachloroplatinate $PtCl_4$ (Sigma-Aldrich) dissolved in 2-propanol. Two 25 μm thick Surlyn ionomer resin films 1702 (DuPont) were employed as the spacer between the electrodes. Two spacers were required in the 2-segment cells (Figure 1) and they were used in the other cells to ease the comparability of the results. Liquid electrolyte consisting of 0.5 M LiI, 0.05 M I_2, and 0.5 M 4-*tert*-butylpyridine in 3-methoxypropionitrile was inserted through the filling channel. The 2-segment cells were filled through the middle hole. Further specifications of the cell components and preparation are shown elsewhere.[7]

In this study, complete solar cells, substrate - counter electrode (SU-CE) cells,[7] counter electrode - counter electrode (CE-CE) cells, and their combinations in 2-segment cells were prepared. 2-segment cells composed of two glass segments were also prepared as a reference to StS PE – glass PE 2-segment cells to exclude the effect of segmentation to the results. In order to make the substrates to resemble the PE substrate in all the SU-CE, they were thermally treated the same way as the PEs at 450 °C for 30 min and dyed since those treatments change electrochemical properties of the substrate.[24-25]

Measurements. Photovoltaic measurements were performed using a solar simulator providing 1000 W/m^2 AM1.5G equivalent light intensity determined by a calibrated silicon reference cell with spectral filters to mimic typical DSC response. The polarization curves were measured using a Keithley 2420 SourceMeter. The solar cells were provided with black masks with a slightly larger aperture size

compared to the active area since this gives most reliable results.[26] The measurement platform was also black.

In the open circuit voltage decay (OCVD) measurements,[27] the cells were illuminated using a red LED (λ_{peak} = 639 nm) which was then turned off. The open circuit voltage was recorded in 5 ms intervals using an Agilent 34970A data logger with input impedance larger than 10 GΩ. The measurements were performed in a black box to exclude stray light.

Electrochemical impedance spectroscopy (EIS) was performed twice over the frequency range 100 mHz – 100 kHz with Zahner Elektrik's IM6 Impedance Measurement unit. The same equipment was also employed in the polarization curves in dark. The EIS measurements were performed in dark in potentiostatic mode at voltages between 0 and -0.7 V using 10 mV amplitude. The equivalent circuit analysis of the data was done with ZView2 software. The EIS data was analyzed similarly as in our previous study; for instance the equivalent circuits were the same.[7]

Surface morphology and elemental composition analysis of the aged cells was made with Zeiss Ultra 55 field emission scanning electron microscope (SEM) with Bruker AXS energy dispersive X-ray spectroscopy (EDS) equipment combined with Quantax 400 software. A 15 kV accelerating voltage was employed in these measurements. The aged cells were dismantled for this analysis.

We detected that the StS PE cells suffered from rapid degradation (within few hours) under 1 sun illumination. In dark, the cells remained stable for a longer period of time. To slow down the degradation and hence leaving time for the measurements, the cells were kept in dark and measured at intervals of a few days. Note that the response time of 2-segment cells is ca. one day as mentioned earlier.

Results and discussion

Initial performance. The initial photovoltaic performance of StS cells was described in detail in our previous work [7] and the initial data presented here (Table 1) is in good correspondence with that. In the case of the StS PE cells, a 10 % decrease in the short circuit current densities (i_{SC}) compared to the previous study [7] is obtained here due to increased optical losses by the thicker bulk electrolyte layer and

increased recombination due to larger triiodide concentration. The fill factor of the StS CE cells is larger than that in the previous study.[7] This is due to batch to batch differences; for instance StS CEs may be more sensitive to slight changes in the thermal treatment than glass CEs.

Table 1. Average initial solar cell performance characteristics and their standard deviations under illumination corresponding to AM1.5G conditions.

	V_{OC} / mV	i_{SC} / mAcm^{-2}	*FF* / %	η / %
StS PE	-643 ± 6	10.5 ± 0.4	52 ± 2	3.48 ± 0.04
StS CE	-681 ± 10	13.6 ± 0.6	48 ± 3	4.7 ± 0.2
Glass, PE light	-666 ± 10	12.8 ± 0.3	57 ± 2	4.87 ± 0.08
Glass, CE light	-636 ± 9	10.7 ± 0.3	62 ± 1	4.21 ± 0.05

Degradation of photovoltaic performance. The efficiency (η) of the StS PE cells dropped approximately 90 % in two weeks in the dark degradation test (Figure 3). The decrease of η of StS PE cells was mostly due to the lowering of i_{SC}. Contrary to StS PE cells, the photovoltaic parameters of the StS CE cells and glass cells remained practically constant after the second measurement day (Figure 3). According to literature StS CEs also age when kept under illumination for weeks.[5] Comparison of the StS PE and CE cells, however, proves that the rapid degradation of the StS PE cells cannot be due to either mere presence of StS in the cell or the encapsulation of StS cells.

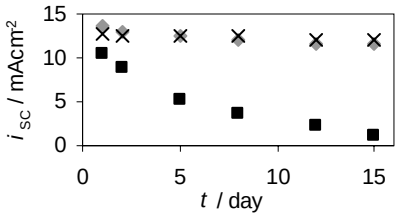

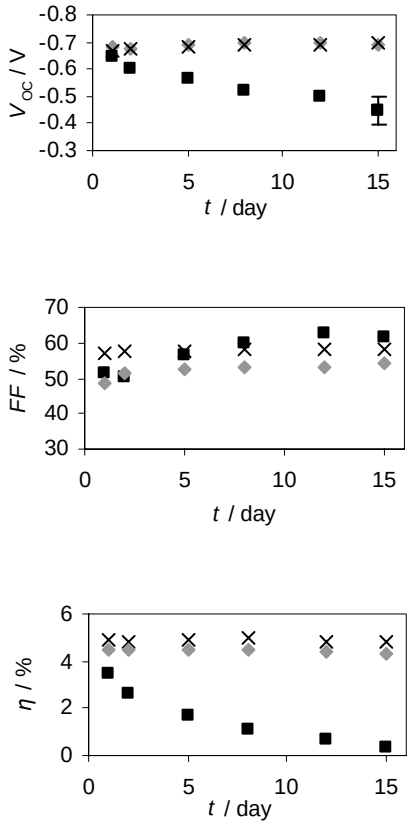

Figure 3. Ageing data of StS PE (black square), StS CE (gray diamond), and glass (black cross) dye solar cells in dark. The data presents average values of 3 cells. The errorbars describing the standard deviation are shown only when larger than the marker size (only one point).

There were no visible changes in the StS PE cells during the measurement period. Since the concentration of triiodide is associated with the appearance (i.e. color), we can conclude that there were no significant changes in it. If there is a decrease in i_{SC} due to the loss of triiodide, the decrease in the triiodide concentration should be roughly corresponding to that in i_{SC}. Hence, the decrease of the StS PE cell i_{SC} cannot be linked with the loss of triiodide due to corrosion (cf. reaction between copper and electrolyte discussed earlier).

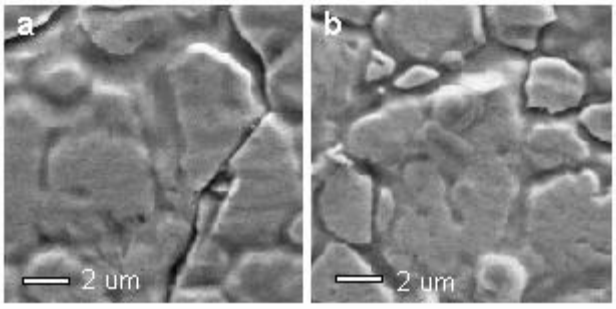

Figure 4. SEM images of a) untreated StS and b) StS PE substrate of an aged cell.

In the SEM, the surface morphology of the StS PE substrate did not differ from that of the untreated StS (Figure 4) which also implies that there is no general corrosion and related pit holes. In addition, EDS composition analysis showed no changes in the composition of the StS PE substrate nor in the dyed TiO_2 layer. The EDS results are, however, indicative only and show that there were no very large changes due to measurement restrictions. For instance, the detection of a monolayer is difficult with EDS meaning that the dye on the TiO_2 could hardly be detected in spite of high coverage.

The fill factor of the StS PE cells did not decrease (Figure 3) which implies that components that primarily affect it, such as the ohmic series resistance of the cell and the charge transfer at the CE cannot be responsible for the deterioration of the StS PE cells. This was also confirmed with EIS measurements (data not shown).

Electron recombination. Since both V_{OC} and i_{SC} of StS PE cells decreased in the aging tests, the degradation might be due to increased electron recombination at the photoelectrode since it can affect i_{SC} in addition to V_{OC}. The effective electron lifetime τ_{eff} at the StS PE measured with OCVD (Figure 5a) and the recombination resistance at the photoelectrode R_{PE} (Figure 6a) decreased throughout the studied voltage range rather simultaneously as function of time whereas the glass cells gave approximately stable values (Figures 5b and 6d). Typically, electron recombination at high voltages is mainly due to recombination via the dyed TiO_2 photoelectrode film and at low voltages via the photoelectrode

substrate,[29-30] and hence the result suggests that there would be changes in both the TiO_2 layer and in the StS substrate.

τ_{eff} is linked with R_{PE} as follows [28]

$$t_{eff} = R_{PE} C_{PE} \quad (3)$$

where C_{PE} in the capacitance at the PE / electrolyte interface. The τ_{eff} values calculated from the EIS data (Figure 6c) according to eq (3) indicate quite similar decrease as those measured with OCVD (Figure 5a) in the case of StS PE cells. The absolute τ_{eff} values of the StS PE cells are, however, about an order of magnitude lower with EIS compared to OCVD (Figures 5a and 6c). In contrast to this, the glass cells give very good correspondence of τ_{eff} between the methods (Figures 5b and 6f). The difference between EIS and OCVD in the small τ_{eff} values is known also in literature [7,27] and possible reasons for this are discussed in our previous publication.[7]

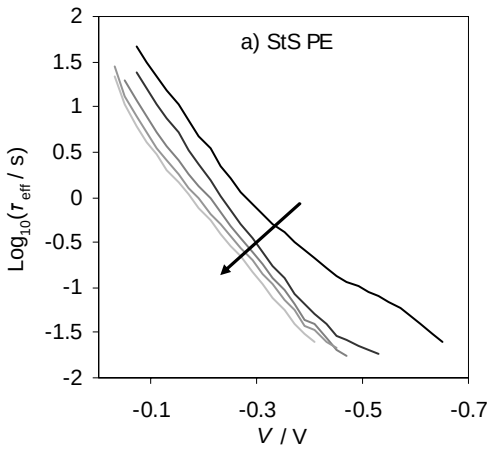

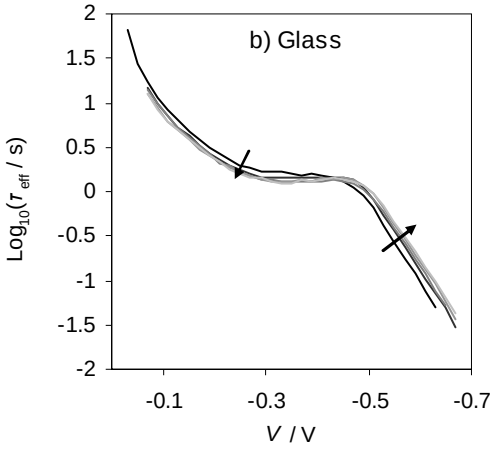

Figure 5. Change of the effective electron lifetimes measured by OCVD at the photoelectrode as a function of time (indicated by arrows) for a) StS PE and b) glass cells. The measurements were taken 1, 5, 8, 12, and 15 days after cell preparation corresponding to the line color changes from black to light gray, respectively.

The capacitance at both the StS PE and glass PE stay approximately constant (Figures 6b and 6e) except for the voltage point -0.6 V. This means that there are no changes in the energetic distribution and density of electron trap states in the photoelectrode.

The initial τ_{eff} values (Figure 5) and the R_{PE} values of the StS PEs (Figure 6) were much lower at the high voltages compared to those at the glass PEs. At the high voltages the data should correspond to the TiO_2 layer.[29-30] In principle the similarly prepared dyed TiO_2 layer should give equal performance. Hence, the StS PE substrate appears to have affected the TiO_2 layer as indicated also in our previous study.[7] The fact that the electron lifetime continued its decrease over the whole observation period (15 days) (Figure 5a) suggests that the decrease seen in the first measurements was due to degradation and not a permanent characteristic difference between the StS and glass substrates.

It is also worth commenting that R_{PE} is directly linked with the photovoltaic curve and hence also with the cell efficiency while τ_{eff} in itself is related to transient (AC) behavior of the cell. The τ_{eff} values measured with OCVD give, however, easily and directly information about the PE. Since the OCVD

measurements are performed in open circuit, the measured voltage corresponds therefore to the voltage over the photoelectrode. EIS measurements are more time consuming and, when measuring as a function of voltage, there is a current flow through the cell which leads to the measured voltage being divided between the cell components. Previously, we have shown how to correct the measured voltage to correspond to the voltage over a single component.[7] Here, such calculations could not be carried out since they require sufficiently stable cell, and those conditions could not be met here due to the degradation of the StS PE cells during the measurements, in particular at the end of the studied time period. Although the R_{PE} values are here compared as function of cell voltage and not the voltage over the PE, it was estimated that it should not affect the interpretation of the data in this case.

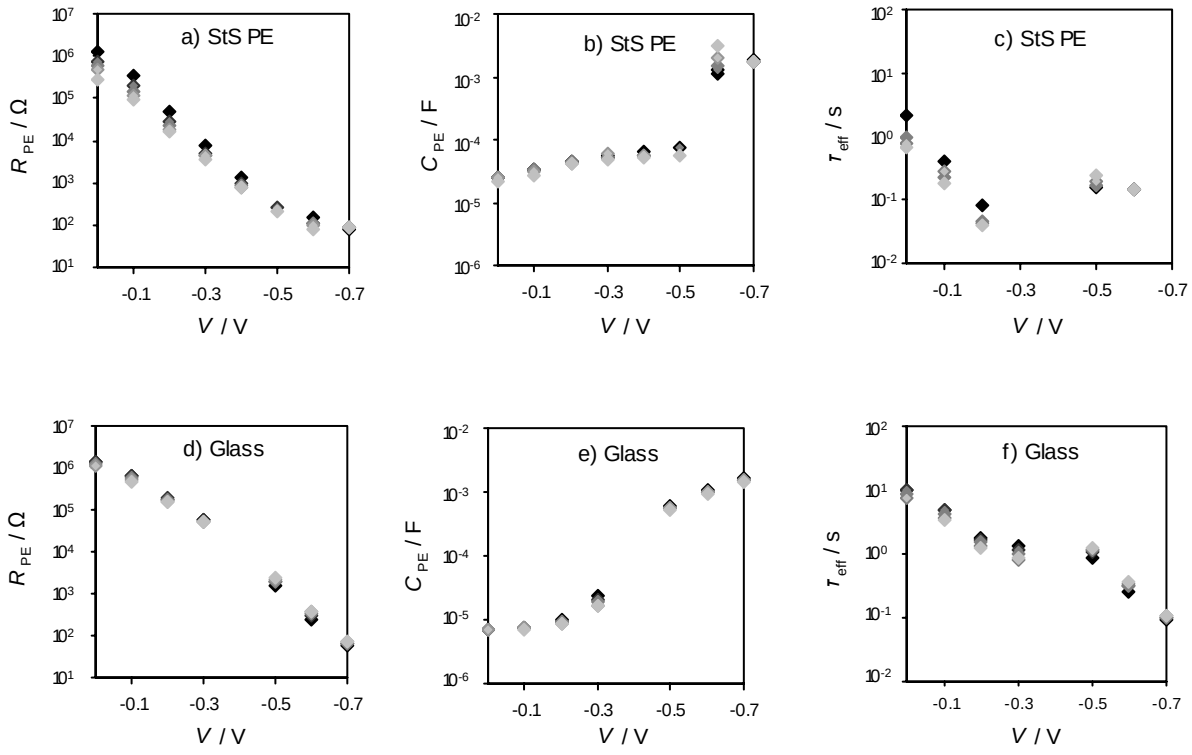

Figure 6. Resistance at the photoelectrode R_{PE}, capacitance at the photoelectrode C_{PE}, and electron lifetime τ_{eff} for StS PE (a, b, c) and glass cells (d, e, f) according to EIS measurements in the dark. The measurements were taken 1, 5, 8, 12, and 15 days after cell preparation and the marker color changes from black to light gray, respectively.

2-segment cells. The decreased recombination resistance of the PE in the case of the StS PE cell suggests that the StS PE substrate might have contaminated the cell with harmful metal oxides or reacted with the electrolyte in a way that does not affect the appearance of the cell. The amount of harmful metal oxides needed to cause a decrease in cell performance is small.[15] If this kind of small amount of metal oxides appeared as sub-nano range particles, their detection would be outside the measurement range of both the SEM and the EDS systems. Hence, the contamination hypothesis cannot be completely eliminated with the preceding SEM and EDS analyses. To examine these kinds of changes, 2-segment cells were prepared. The idea was to determine whether or not a StS PE can contaminate a glass PE via electrolyte. Here, we focus on changes in i_{SC} since that characteristic was primary affected in the degradation of StS PE cells.

The decrease of StS PE segment i_{SC} was similar as in normal StS PE cells (Figure 3 and 7). The performance of the glass segment which was connected to the StS PE segment did not differ from that of a glass segment connected to another glass segment in dark degradation test which lasted almost 20 days (Figure 7). In the experimental section it was showed that changes in one segment should affect the other segment already in a day.

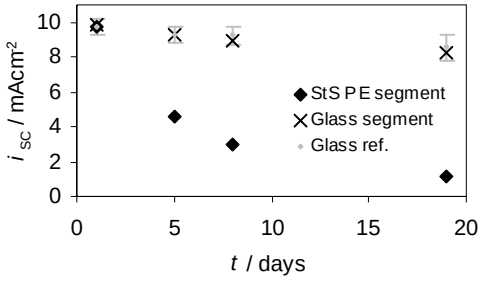

Figure 7. i_{SC} of StS PE segment (black diamond) and that of a glass segment (black cross) connected to it. i_{SC} of glass – glass 2-segment (gray dot) is also presented as a reference. The cells were illuminated

from the CE side. The values represent the average of 3 segments. The error bars indicate the standard deviation and they are marked when larger than the marker size.

However, it is in principle possible that the effect is electrolyte mediated, but adsorption of the contaminating material on the nanoporous high surface area TiO_2 photoelectrode film StS PE prevents its transfer from the StS PE segment to the glass segment, cf. adsorption of 4-tBP.[16] To investigate this hypothesis, the TiO_2 film was ruled out by preparing 2-segment cells where the StS PE was replaced with a bare StS substrate. Mere presence of a StS substrate does not itself cause the instability as can be deduced from the StS CE cell data (Figure 3). This is why additional stimulus such as polarization is required in order to have a possibility to evoke degradation effects. Hence, the StS substrate was polarized to -0.5 V to mimic the polarization of a StS PE to result in similar StS substrate/electrolyte interaction as in illuminated StS PE cells. The polarized StS substrates did not affect the i_{SC} of the glass segment either in this test which also lasted about 20 days (data not shown).

Hence, apparently the electrolyte was not contaminated nor was subjected to other significant changes that would itself lead to the rapid degradation of the StS PE cells. If there is contamination from the StS substrate to the TiO_2 layer, it could transfer from the StS substrate to the TiO_2 for instance by surface diffusion without the electrolyte. If the electrolyte has reacted with the stainless steel, it needs to have had a major influence on the performance of StS substrate, for instance the contact between the StS and the TiO_2 layer, while leading to a very minor difference in the electrolyte. The analysis of these other possible aging mechanism is, however, out of the scope of this study since here the focus is on the electrolyte.

Conclusions

A stainless steel photoelectrode dye solar cell suffers from rapid degradation within few days. This does not occur in a stainless steel counter electrode cell. There were no simultaneous visual changes associated with the aging of the StS PE cells indicating that their degradation is not due to loss of

triiodide in the electrolyte e.g. through corrosion reactions. The OCVD and EIS measurements showed decreased electron lifetime and recombination resistance at the stainless steel photoelectrode.

To investigate the role of the electrolyte in such a rapid degradation process, 2-segment cells were used connecting laterally a glass based DSC with a stainless steel DSC via a common electrolyte layer. The segment cell method is a non-destructive way to decouple electrolyte mediated degradation phenomena from local one as well as their effect on different cell components during long term stability testing. Measurements with 2-segment cells confirmed that during the rapid degradation of the stainless steel cells no significant degradation appears in the electrolyte. We may thus conclude that the electrolyte contamination is not the reason for the degradation in stainless steel dye solar cells.

Acknowledgements

The study was funded by the Academy of Finland. K. M. and J.H. are grateful for the scholarships of the Graduate School of Energy Technology. We thank Tapio Saukkonen (Department of Engineering Design and Production, TKK) for the SEM images and the EDS analysis.

References

(1) Kroon, J. M.; Bakker, N. J.; Smit, H. J. P.; Liska, P.; Thampi, K. R.; Wang, P.; Zakeeruddin, S. M.; Grätzel, M.; Hinsch, A.; Hore, S.; Würfel, U.; Sastrawan, R.; Durrant, J. R.; Palomares, E.; Pettersson, H.; Gruszecki, T.; Walter, J.; Skupien, K.; Tulloch, G. E., *Prog. Photovolt: Res. Appl.* **2007**, 15, 1-18.

(2) Zweibel, K., *Sol. Energy Mater. Sol. Cells* **1999**, 59, 1-18.

(3) Payne, A.; Duke, R.; Williams, R. H., *Energy Policy* **2001**, 29, 787-800.

(4) Toivola, M.; Ahlskog, F.; Lund, P., *Sol. Energy Mater. Sol. Cells* **2006**, 90, 2881-2893.

(5) Ma, T.; Fang, X.; Akiyama M.; Inoue K.; Noma H.; Abe E., *J. Electroanal. Chem.* **2004**, 574, 77-83.

(6) Fang, X.; Ma, T.; Akiyama M.; Guan, G.; Tsunematsu, S.; Abe, E., *Thin Solid Films* **2005**, 472, 242-245.

(7) Miettunen, K.; Halme, J.; Toivola, M.; Lund, P., *J. Phys.Chem. C* **2008**, 112, 4011-4017.

(8) Murakami, T.N.; Grätzel, M., *Inorg. Chim. Acta* **2008**, 361, 572-580.

(9) Kang, M. G.; Park, N.-G.; Ryu, K. S.; Chang, S. H.; Kim, K.-J., *Chemistry Letters* **2005**, 34, 804-805.

(10) Kang, M. G.; Park, N.-G.; Ryu, K. S.; Chang, S. H.; Kim, K.-J., *Sol. Energy Mater. Sol. Cells* **2006**, 90, 574-581.

(11) Jun, Y.; Kim, J.; Kang, M. G., *Sol. Energy Mater. Sol. Cells* **2007**, 91, 779-784.

(12) Onoda, K.; Ngamsinlapasathian, S.; Fujieda, T.; Yoshikawa, S., *Sol. Energy Mater. Sol. Cells* **2007**, 91, 1176-1181.

(13) Park, J. H.; Jun, Y.; Yun, H.-G.; Lee, S.-Y.; Kang, M. G., *J. Electrochem. Soc.* **2008**, 155, F145-F149.

(14) Miettunen, K.; Toivola, M.; Halme, J.; Armentia, J.; Vahermaa, P.; Lund, P., *Proceedings of 22nd European Photovoltaic Solar Energy Conference and Exhibition*, **2007**.

(15) Kay, A., PhD Thesis, Ecole Polytechnique Fédérale de Lausanne, Switzerland, **1994**.

(16) Miettunen, K.; Halme, J.; Lund, P., *Electrochem. Comm.* **2009**, 11, 25-27.

(17) Zaban, A.; Zhang, J.; Diamant, Y., Melemed, O.; Bisquert J., *J. Phys. Chem. B* **2003**, 107, 6022-6025.

(18) Ofir, A.; Grinis, L.; Zaban, A., *J. Phys. Chem. C* **2008**, 112, 2779-2783.

(19) Papageorgiou, N.; Athanassov, Y.; Armand, M.; Bonhote, P.; Pettersson, H.; Azam, A.; Grätzel, M., *J. Electrochem. Soc.* **1996**, 143, 3099-3108.

(20) Kay, A.; Grätzel, M., *Sol. Energy Mater. Sol. Cells* **1996**, 44, 99-117.

(21) Balluffi, R. W.; Allen, S. M.; Carter, W. C., *Kinetics of Materials*, John Wiley & Sons, Inc, **2005**.

(22) Hauch, A.; Georg, A., *Electrochem. Acta* **2001**, 46, 3457-3466.

(23) Papageorgiou, N.; Maier, W. F.; Grätzel, M., *J. Electrochem. Soc.* **1997**, 144, 876-884.

(24) Cameron, P. J.; Peter, L. M.; Hore, S., *J. Phys. Chem. B* **2005**, 109, 930-936.

(25) Sastrawan, R.; Renz, J.; Prahl, C.; Beier, J.; Hinsch, A.; Kern, R., *J. Photochem. Photobiol. A - Chem.* **2006**, 178, 33-40.

(26) Ito, S.; Nazeeruddin, K.; Liska, P.; Comte, P.; Charvet, R.; Péchy, P.; Jirousek, M.; Kay, A.; Zakeeruddin, S.; Grätzel, M., *Prog. Photovolt: Res. Appl.* **2006**, 14, 581-601.

(27) Zaban, A.; Greenshtein, M.; Bisquert, J., *ChemPhysChem* **2003**, 4, 859-864.

(28) Bisquert, J.; Garcia-Belmonte, G.; Fabregat-Santiago, F.; Ferriols, N. S.; Bogdanoff, P.; Pereira, E., *J. Phys. Chem. B* **2000**, 104, 2287-2298.

(29) Fabregat-Santiago, F.; Bisquert, J.; Garcia-Belmonte, G.; Boschloo, G.; Hagfeldt, A., *Sol. Energy Mater. Sol. Cells* **2005**, 87, 117-131.

(30) Cameron, P. J.; Peter, L. M., *J. Phys. Chem. B* **2005**, 109, 7392-7398.